9.8 A COMPARISON OF WAVE-INDUCED RESIDUAL AND LAGRANGIAN TRANSPORT IN THE STRATOSPHERE

D. Pendlebury* and T. G. Shepherd
University of Toronto, Toronto, Canada

1 INTRODUCTION

Observations of long-lived tracers, such as N_2O (Randel et al. 1993), reveal the nature of the mean meridional transport in the stratosphere. The so-called Brewer-Dobson circulation consists of an ascending branch of air in the tropics and descending branches at the poles. Although the timescale for a particle to move through the stratosphere depends on the path of the particle, the overturning time of the stratosphere via the Brewer-Dobson circulation is approximately 5-10 years.

Temperature measurements of the stratosphere indicate that the temperature at tropical latitudes is lower than that which would be expected from radiative arguments. Similarly, the temperature at extratropical latitudes is higher than expected, particularly in the northern hemisphere winter. This departure from radiative equilibrium implies that the observed poleward circulation is thermally indirect and therefore must be mechanically driven.

The driving mechanism behind the Brewer-Dobson circulation at midlatitudes is planetary-wave forcing. Planetary waves produced in the troposphere propagate into the stratosphere where they break and dissipate. The deposition of wave momentum at midlatitudes provides a mechanism for the redistribution of angular momentum, which drives the poleward circulation. The upwelling in the tropics and downwelling near the poles is then a result of mass continuity.

While this picture of the circulation seems complete, there are many assumptions in the theory. The mathematical connection between dissipation of planetary-wave momentum and poleward mass transport exists only for flow that is quasigeostrophic and steady, but more notably, the disturbances must also be small-amplitude and linear. In particular, in order for the transport and TEM velocities to be formally the same, the waves must be steady, adiabatic, quasigeostrophic, linear and small-amplitude. However, the process of wave breaking and the subsequent cascade of enstrophy to smaller scales, where three-dimensional turbulence leading to molecular diffusion is ultimately responsible for the dissipation of the waves, is a highly nonlinear process. This is well established through the theory of Rossby-wave critical layers (McIntyre and Palmer 1983).

*Corresponding author address: D. Pendlebury, Univ. of Toronto, Department of Physics, Toronto, Canada, M5S 1A7; e-mail: diane@atmosp.physics.utoronto.ca

2 THEORY

To describe tracer transport the most natural framework is the Lagrangian mean. However, this can be difficult to describe mathematically. Instead, a hybrid Eulerian-Lagrangian mean, the Generalized Lagrangian Mean (GLM), has been defined by (Andrews and McIntyre 1978). In the GLM framework, a conservative tracer is advected by the Lagrangian mean winds, but there is no eddy flux of the tracer, as in the Eulerian mean framework. For the special case of linear waves, the GLM and the Eulerian mean is the Stokes correction and can be viewed as a correction to the mean flow. It can be nonzero even in oscillatory, small-amplitude flow (Matsuno 1980).

The GLM is useful for studying the transport of air parcels since it is also valid for large amplitude disturbances. However, in practice, GLM theory is not used because complications can arise, even with small-amplitude disturbances. For example, $\vec{u}^L$ is generally divergent even for an incompressible fluid (Andrews and McIntyre 1978). Furthermore, if the flow is very nonlinear, it is possible for the material contours to evolve chaotically, making it impossible to find the backwards map to Eulerian space, so that while transport can be described in the GLM space, meaning cannot be attributed to the transport in real space.

An alternative diagnostic is the Transformed Eulerian Mean (TEM) framework (Andrews et al. 1987). In the TEM framework, the eddy forcing in the zonal momentum equation can be written as the Eliassen-Palm (EP) flux divergence, $\vec{\nabla} \cdot \vec{F}$. In regions of planetary-wave dissipation, such as the stratosphere, the EP flux divergence is generally negative leading to a poleward $\bar{v}^*$ in both hemispheres. Also, the remaining flux terms in the thermodynamic equation tend to be small in the atmosphere so that the main balance is between the diabatic heating Q and $\bar{\omega}^* \frac{\partial \bar{\theta}}{\partial p}$ in the steady state limit. In this way the TEM circulation is close to the diabatic circulation.

In a quasigeostrophic approximation, the difference between the residual and Eulerian mean velocities is equivalent to the Stokes drift (Dunkerton 1978; Mo and McIntyre 1997). In this way the TEM circulation can be viewed as a surrogate for the Lagrangian mean circulation. However, this requires that the waves be small-amplitude and that nonconservative transient effects be negligible. It is under these generally unrealistic assumptions that the residual velocities and Lagrangian velocities can be shown to be equivalent.

3 MODEL RESULTS

3.1 Model Setup

The model solves the primitive equations for a dry, rotating, spherical atmosphere. The horizontal spectral truncation uses 42 wavenumbers in the meridional direction and 10 wavenumbers in the zonal direction. The vertical discretization uses 60 pressure levels spaced almost equally in log-pressure height with a resolution of approximately 1.25 km in the interior of the model and a lower boundary at 200 mb.

Dissipation in the model is included in the form of ∇^8 hyperdiffusion and a second order vertical viscosity which act only on the deviation from the initial background state. Newtonian cooling relaxes the potential temperature back to the specified radiative equilibrium temperature, and Rayleigh friction is optionally included and acts only on the waves. A sponge layer is used above 70 km in order to dissipate waves in this region and prevent reflection off the upper boundary. The sponge is nonzonal to avoid spurious feedbacks (Shepherd et al. 1996).

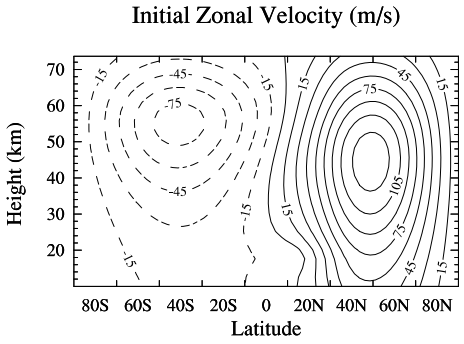

Figure 1: The initial wind field for both runs. Contour levels are 15 m/s.

The initial conditions of the model are set such that the background wind is similar to northern hemisphere winter solstice conditions (Figure 1). The potential temperature field is then calculated by using gradient wind balance. The background vertical (globally averaged) stratification is chosen to be isothermal with a scale height of 7 km which yields a buoyancy frequency of $2 \times 10^{-2} s^{-1}$. Stationary planetary waves are generated at the lower boundary by specifying the geopotential Φ'_S. The forcing is turned on over the first 10 days and the model is then run until it reaches a statistical steady state. The diagnostic quantities are time averaged over the last 60 days of the run.

The transport velocities are calculated by using an off-line particle advection scheme adapted from a contour advection code by Norton and Dritschel. The particle advection is performed over the same 60 days used to calculate the diagnostics. The winds are saved every 12 hours and projected onto isentropic surfaces. Diabatic vertical advection was added by using the diabatic heating field calculated from the model.

3.2 Transport vs. Residual Circulation

The first case shown is for a weakly nonlinear regime, with a small-amplitude forcing and a Rayleigh friction timescale of 10 days. Despite the weak forcing, a narrow surf zone still develops (see Figure 2), centered on the zero-wind line; this is a weakly nonlinear Rossby-wave critical layer. The EP flux divergence, shown in Figure 4, is negative as expected and does not extend into the SH, as expected for stationary waves. The second case is in a strongly nonlinear regime and has a larger amplitude forcing with no Rayleigh friction. In both cases, the Newtonian cooling coefficient is set to 10 days and the zonal wavenumber of the forcing function is m=2.

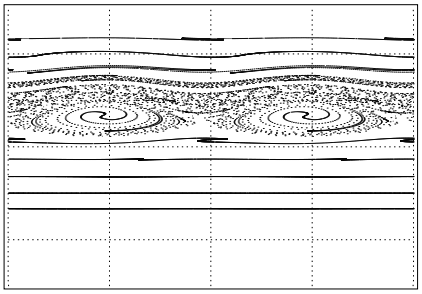

Figure 2: Particle advection at 60 day on the 1000K surface for the weakly nonlinear case. The latitude range extends from pole to pole.

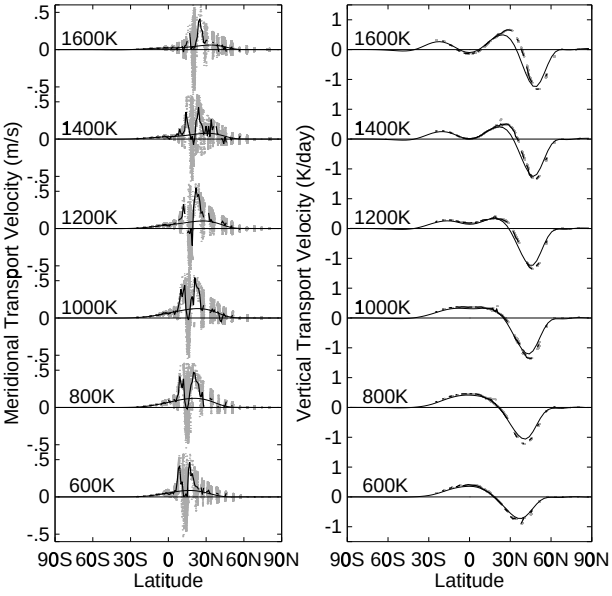

Figure 3: Transport velocities and residual velocities for the weakly nonlinear case for several isentropic surfaces. The meridional velocities are shown on the left panel and vertical velocities, in isentropic coordinates, are on the right.

The transport velocity of each particle is calculated

as

$$v^T = \frac{a\pi}{180}\frac{\varphi_f - \varphi_i}{t_f - t_i}, \qquad w^T = \frac{\theta_f - \theta_i}{t_f - t_i}. \tag{1}$$

Each particle must be associated with a latitude and height. This is accomplished by taking the Lagrangian average of each particle position in both latitude and height.

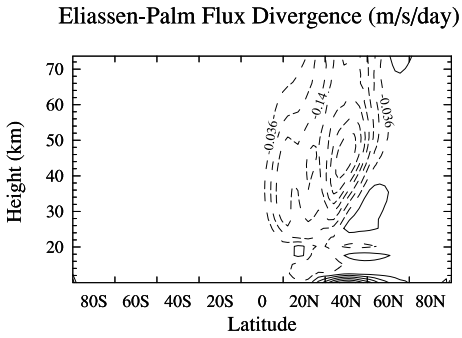

Figure 4: The EP flux divergence for the weakly nonlinear case. Contour levels are 0.052 m/s/day.

Figure 3 shows the transport velocities calculated from the offline particle advection and the residual velocities calculated from the model results, for the weakly nonlinear case. The left panel shows the meridional velocities and the right shows the vertical velocities, calculated in θ coordinates. Transport velocities of individual particles are shown as grey dots, the zonal mean of the transport velocities is represented by the thick line and the residual velocity is the thin line. Gaps in the meridional representation of the transport velocities are due to a lack of particles associated with that latitude and isentropic surface.

Table 1: Approximate height of isentropic surfaces.

1600K	56km	1400K	53km
1200K	50km	1000K	45km
800K	40km	600K	32km

The surf zone is clearly visible in the meridional velocity plot, distinguished by the cloud of dots centered on it. This cloud is a result of particles trapped inside the surf zone, which are travelling back and forth between the two transport barriers. On average, most of the particles in the surf zone will be associated with the center of the surf zone in a Lagrangian sense, and their meridional transport velocity will be close to zero. Surrounding this zero, the zonal average of the transport velocities shows two peaks, also inside the surf zone. The peak near the southern edge of the surf zone is created by particles that have spent the first part of the integration south of the surf zone and then moved into the surf zone for the second part of the integration. This means that the mean velocities of these particles are relatively large and the positions associated with the particles are between the two regions. The peak near the northern edge is created in the same way by particles that begin inside the surf zone and are transported north of the surf zone during the integration. These results imply a systematic northward transport of particles, however it is not uniform as suggested by the residual velocity. It can be clearly seen that inside the surf zone the transport and residual velocities do not agree.

Outside of the surf zone, the transport and residual velocities agree very well. This is expected since this is a region of linear, non-breaking waves. In these regions, the distribution of particle velocities about the zonal-mean transport velocity is due to the fact that the particles are initialized on latitude circles, which are not conserved. This promotes a spreading of the particles off the original latitude in both directions. This spreading is not, however, associated with the irreversible transport of particles, as can be seen in Figure 2. The vertical velocities for the weakly nonlinear case agree very well between the transport and residual circulations everywhere, and there is very little spread of particle velocities from the zonal mean.

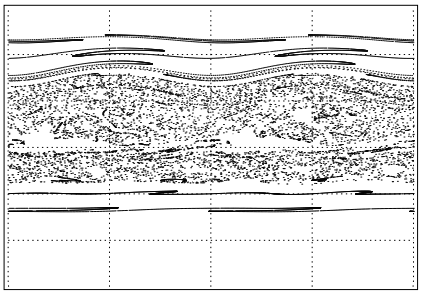

Figure 5: As for Figure 2 but on the 1200K surface for the strongly nonlinear case.

Figure 6 shows the transport and residual velocities for the strongly nonlinear case. Below the 1000K surface, the results are very similar to the weakly nonlinear case. There is a clear surf zone, although larger than in Figure 3 (see also Figure 5), and the two peaks near the edge of the surf zone are similar. Again, the residual and transport velocities agree reasonably well outside the surf zone and do not agree inside the surf zone.

At and above 1000K, however, the results are very different. This region is anomalous in that it has a positive EP flux divergence (Figure 7), suggesting that this is a region of wave generation instead of dissipation. Indeed, a wave with a period of 2 days has appeared over the equator, possibly generated by an inertial-like instability. The presence of a nonzero EP flux divergence in the SH also suggests that nonstationary waves must be present. The residual circulation in Figure 6 has also changed sign in the tropics, as predicted by TEM theory. The meridional transport velocities, however, seem to average to zero. The cloud of grey dots has also grown suggesting that the mixing region has broadened. In fact, the surf zone in the NH is still intact but another region of mixing in the SH has developed (see Figure 5), indicating that non-stationary

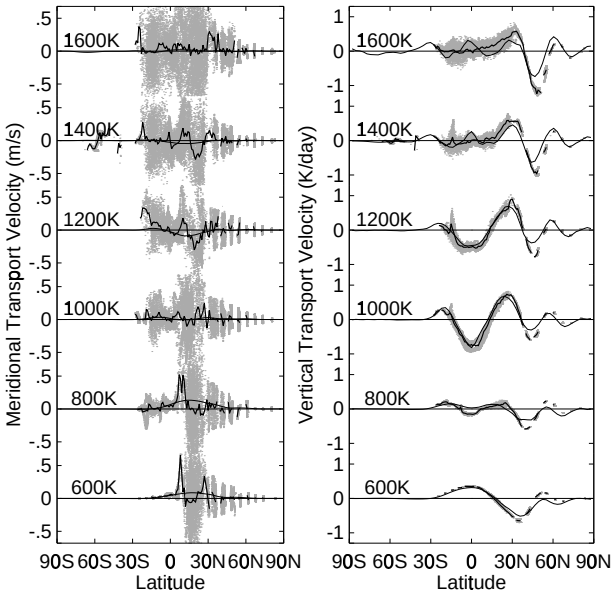

Figure 6: Same as in Figure 3 but for the strongly nonlinear case.

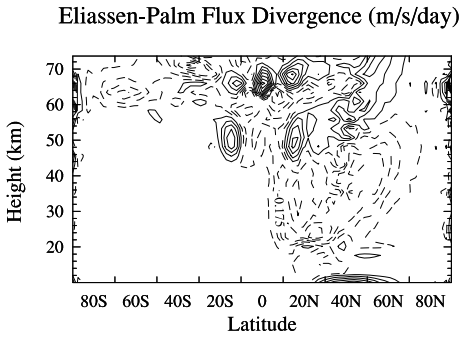

Figure 7: The EP flux divergence for the strongly nonlinear case. Contour levels are 0.075 m/s/day.

waves are present.

The vertical velocities in this case do not agree as well as they do in the weakly nonlinear case. Below 1000K there is generally good agreement between the residual and transport velocities. However at higher altitudes, although the velocities are still of the same sign in most regions, the residual velocity is never as negative as $\overline{w}^T$ in the downwelling regions near 40N. The vertical velocities of individual particles also show a much larger spread of velocities about the zonal mean. This is due to the development of smaller scales of the diabatic heating field through wavebreaking, which creates diabatic dispersion of the particles (Sparling et al. 1997).

4 CONCLUSIONS

The theory of the Brewer-Dobson circulation seems to work well in regions of linear, non-breaking waves, as expected. However, in regions of overturning and wavebreaking, such as the surf zone, the theory breaks down.

The vertical transport and residual velocities agree very well in the weakly nonlinear case, and agree reasonably well in most regions of the strongly nonlinear case. This is because the vertical particle advection can be described in isentropic coordinates where movement off an isentropic surface corresponds to a diabatic, nonconservative process and not to a reversible undulation of a pressure surface. In the meridional direction, however, the particle advection is described in latitude coordinates and is therefore exhibits both reversible and irreversible effects. There is no natural Lagrangian coordinate analogous to θ in the meridional direction since the only possible candidate, equivalent latitude, does not provide a good meridional coordinate in the surf zone.

REFERENCES

Andrews, D. G., J. R. Holton, and C. B. Leovy (1987). *Middle Atmosphere Dynamics*, Volume 40 of *International Geophysical Series*. Academic Press, Inc.

Andrews, D. G. and M. E. McIntyre (1978). An exact theory of nonlinear waves on a Lagrangian-mean flow. *J. Fluid Mech. 89*, 609–646.

Dunkerton, T. J. (1978). On the mean meridional mass motions of the stratosphere and mesosphere. *J. Atmos. Sci. 35*, 2325–2333.

Matsuno, T. (1980). Lagrangian motion of air parcels in the stratosphere in the presence of planetary waves. *Pure Appl. Geophys. 118*, 189–216.

McIntyre, M. E. and T. N. Palmer (1983). Breaking planetary waves in the stratosphere. *Nature 305*, 593–600.

Mo, R. and M. E. McIntyre (1997). On anomalous meridional circulations and Eliassen-Palm flux divergences in an idealized model of dissipating, nonbreaking Rossby waves. *Dyn. Atmos. Oceans 27*, 575–600.

Randel, W. J., J. C. Gille, A. E. Roche, J. B. Kumer, J. L. Mergenthaler, J. W. Waters, E. F. Fishbein, and W. A. Lahoz (1993). Stratospheric transport from the tropics to middle latitudes by planetary-wave mixing. *Nature 365*, 533–5.

Shepherd, T. G., K. Semeniuk, and J. N. Koshyk (1996). Sponge layer feedbacks in middle-atmosphere models. *J. Geophys. Res. 101*, 23,447–23,464.

Sparling, L. C., J. A. Kettleborough, P. H. Haynes, M. E. McIntyre, J. E. Rosenfield, M. R. Schoeberl, and P. A. Newman (1997). Diabatic cross-isnetropic dispersion in the lower stratosphere. *J. Geophys. Res. 102*, 25,817–25,829.